

Progress on the lattice QCD calculation of the rare kaon decay: $K^+ \rightarrow \pi^+ \nu \bar{\nu}$

N. H. Christ*

Department of Physics, Columbia University, New York, NY 10027, USA

E-mail: nhc@phys.columbia.edu

X. Feng

Department of Physics, Columbia University, New York, NY 10027, USA

School of Physics, Peking University, Beijing 100871, China

Center for High Energy Physics, Peking University, Beijing 100871, China

Collaborative Innovation Center of Quantum Matter, Beijing 100871, China

E-mail: pkufengxu@gmail.com

A. Lawson

School of Physics and Astronomy, University of Southampton, Southampton SO17 1BJ, UK

E-mail: allg13@soton.ac.uk

A. Portelli

SUPA, School of Physics, The University of Edinburgh, Edinburgh EH9 3JZ, UK

E-mail: antonin.portelli@me.com

C. Sachrajda

School of Physics and Astronomy, University of Southampton, Southampton SO17 1BJ, UK

E-mail: cts@soton.ac.uk

RBC and UKQCD Collaborations

The rare kaon decay $K^+ \rightarrow \pi^+ \nu \bar{\nu}$ is highly suppressed in the standard model and thus provides an ideal place to search for new physics beyond the standard model. These decays are the principal objective of a new experiment, NA62 at CERN. Another new experiment to search for $K_L \rightarrow \pi^0 \nu \bar{\nu}$ is now underway at J-PARC. Given the goal of 10% precision by NA62, it is important to determine the long-distance contributions to the $K^+ \rightarrow \pi^+ \nu \bar{\nu}$ amplitude with a controlled uncertainty. In this talk we will report the progress on the lattice QCD calculation of the long-distance contributions to the $K^+ \rightarrow \pi^+ \nu \bar{\nu}$ decay amplitude, with an emphasis on the treatment of the short-distance divergence in the bilocal operator product.

34th annual International Symposium on Lattice Field Theory

24-30 July 2016

University of Southampton, UK

*Speaker.

The rare kaon decay $K^+ \rightarrow \pi^+ \nu \bar{\nu}$ is characterized at long distances as resulting from a flavor-changing neutral current and cannot occur at first order in the standard model. Instead the standard model prediction comes from the diagrams shown in Fig. 1 in which two heavy gauge bosons must be exchanged leading to a suppression by four powers of their masses, M_W and M_Z .

The $K^+ \rightarrow \pi^+ \nu \bar{\nu}$ decay and its companion process $K_L \rightarrow \pi^0 \nu \bar{\nu}$ are actively studied as decays that are particularly sensitive to new physics for two reasons. First as second-order weak processes they are strongly suppressed in the standard model, increasing the possible visibility of new phenomena. Second, they are short-distance dominated, allowing the standard model prediction to be determined from the matrix element of a vector current (accurately known from experiment) multiplied by a short-distance, perturbative Wilson coefficient.

Here we focus on the charged kaon decay $K^+ \rightarrow \pi^+ \nu \bar{\nu}$. Of the two rare kaon decays with a two-neutrino final state, the charged decay has the potentially largest long-distance effects which best motivates a lattice QCD study. The NA62 experiment expects to measure the branching ratio of this decay to 10% accuracy in the next few years making it important that potentially-uncertain, non-perturbative, long-distance effects are understood to greater accuracy. This study [1] is part of a larger effort which also includes the rare kaon decays into charged leptons [2, 3].

The standard model prediction for the branching ratio [4] for this decay can be written as:

$$\text{Br} = \kappa_+ (1 + \Delta_{\text{EM}}) \left[\left(\frac{\text{Im}\lambda_t}{\lambda^4} X(x_t) \right)^2 + \left(\frac{\text{Re}\lambda_c}{\lambda} P_c + \frac{\text{Re}\lambda_t}{\lambda^5} X(x_t) \right)^2 \right], \quad (1)$$

where $\lambda_q = V_{qs}^* V_{qd}$ for $q = t, c$ can be written in terms of the CKM matrix elements while $\lambda = |V_{us}|$.

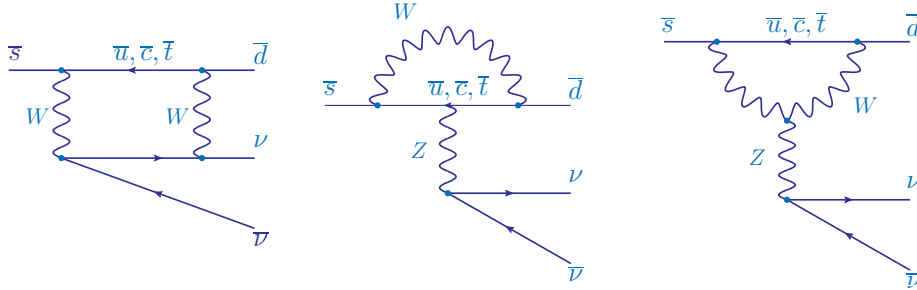


Figure 1: The three types of diagrams contributing to $K^+ \rightarrow \pi^+ \nu \bar{\nu}$ in the standard model. We refer to the left-most and center diagrams as WW - and Z -exchange. We will not explicitly discuss the right-most diagram since this is dominated by short-distance phenomena at the scale of $1/M_W$ and lattice methods are not needed for its evaluation. As is conventional in a lattice QCD discussion, the interactions of the quark propagators with QCD gluons are not shown.

The largest contribution to this charged kaon decay comes from short distances with the top quark alone contributing about 50%. The other 50% comes for the top-charm interference and (charm)² pieces present in the second term in Eq. (1). However, even this relatively large charm contribution also comes from short distances. This can be seen from the left-most diagram shown in Fig. 1. At distances large compared to $1/M_W$, the two W propagators can be reduced to points which results in a quadratically-divergent, quark loop containing two, four-fermion vertices. The GIM cancellation between up and charm and the fact that this divergent behavior is cut off at the W

scale imply a result $\propto (m_c^2 - m_u^2) \ln(M_W^2/m_c^2)/M_W^4$ where m_c and m_u are the masses of the charm and up quark. Since this log contribution necessarily comes from an energy scale larger than m_c , the short distance component of the charm contribution is enhanced by a factor of $\ln(M_W^2/m_c^2) \approx 8.4$ suggesting a long-distance contribution of $50\%/8.4=6\%$. However, this may be an over estimate of the short-distance effects because the contribution of the $\ln(M_W^2/m_c^2)$ piece is reduced by a factor of two when the sums over the leading and next-leading logarithms are included.

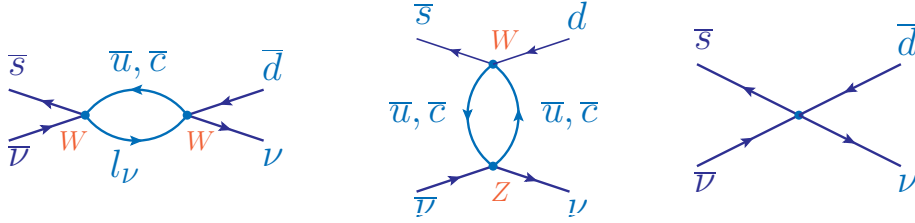


Figure 2: The three types of diagrams providing the long-distance description of $K^+ \rightarrow \pi^+ \nu \bar{\nu}$ decay in the standard model. These diagrams correspond to those shown in Fig. 1 and result when the massive W and Z propagators are treated as local. The right-most diagram receives contributions from all three diagrams in Fig. 1 because the short-distance parts of the left and center diagrams in that figure are not correctly captured by left and center diagrams above and must be corrected by the diagram on the right.

The long-distance contribution which we will compute using lattice QCD can be represented by the three diagrams shown in Fig. 2. These diagrams result from the effective theory which represents the standard model at long distances and is described by the weak Hamiltonian:

$$\mathcal{H}_{\text{eff}} = + \frac{G_F}{\sqrt{2}} \left\{ \sum_{\substack{q=u,c \\ \ell=e,\mu,\tau}} (V_{qs}^* O_{q\ell}^{\Delta S=1} + V_{qd} O_{q\ell}^{\Delta S=0}) + \sum_{\ell=e,\mu,\tau} O_{\ell}^Z + \sum_{q=u,c} \lambda_q O_q^W \right\} + O_0. \quad (2)$$

This expression for \mathcal{H}_{eff} has a hybrid form. The three terms in curly brackets are of order G_F , typically identified as first-order and given by:

$$O_{q\ell}^{\Delta S=1} = C_{\Delta S=1} (\bar{s}q)_{V-A} (\bar{\nu}_{\ell}\ell)_{V-A} \quad O_{q\ell}^{\Delta S=0} = C_{\Delta S=0} (\bar{q}d)_{V-A} (\bar{\ell}\nu_{\ell})_{V-A} \quad (3)$$

$$O_{\ell}^Z = C_Z \sum_{q=u,c,d,s} (T_3^q \bar{q}\gamma_{\mu}(1-\gamma_5)q - Q_{\text{em},q} \sin^2 \theta_W \bar{q}\gamma_{\mu}q) \bar{\nu}_{\ell}\gamma_{\mu}(1-\gamma_5)\nu_{\ell} \quad (4)$$

$$O_q^W = C_1 (\bar{s}_a q_b)_{V-A} (\bar{q}_b d_a)_{V-A} + C_2 (\bar{s}_a q_a)_{V-A} (\bar{q}_b d_b)_{V-A} \quad (5)$$

while the fourth, right-most operator is second-order and has the form

$$O_0 = C_0 \sum_{\ell=e,\mu,\tau} (\bar{s}d)_{V-A} (\bar{\nu}_{\ell}\nu_{\ell})_{V-A}. \quad (6)$$

The operators $O_{q\ell}^{\Delta S=1}$ and $O_{q\ell}^{\Delta S=0}$ of Eq. (3) describe first-order semi-leptonic decays and correspond to the two vertices in the left-most diagram of Fig. 2. The operator O_{ℓ}^Z of Eq. (4) describes a similar lepton-quark coupling coming from Z exchange while the two operators which appear in O_q^W are the usual color-mixed and color-unmixed operators describing non-leptonic kaon decay.

In contrast, the operator O_0 is a two-quark/two-lepton, strangeness-changing neutral current operator which appears at second order in G_F . This operator plays two, closely-related roles in

\mathcal{H}_{eff} . First it represents the short-distance parts of the underlying standard-model processes that contribute to the decay $K^+ \rightarrow \pi^+ \nu \bar{\nu}$. Second it acts as a counter-term that is needed when the operator \mathcal{H}_{eff} is used at second order. As is standard in effective field theory, when the operators introduced into \mathcal{H}_{eff} to describe first-order process are used in a second-order calculation (as is the case in the two left-most diagrams in Fig. 2) new divergences appear that require new counter terms. The operator O_0 plays this role as well. Thus, the Wilson coefficient C_0 , which appears in the definition of O_0 in Eq. (6), contains convention-dependent parts needed to compensate for the regularization scheme introduced to make the second-order diagrams of Fig. 2 well-defined.

1. Lattice QCD formulation

In order to calculate the long-distance contribution to $K^+ \rightarrow \pi^+ \nu \bar{\nu}$ we must overcome two difficulties: i) The appearance of unphysical terms (explained below) in the second-order, Euclidean-space expression for the decay amplitude. ii) The need to renormalize the logarithmic dependence on the lattice cutoff coming from the integration region where the two vertices in the left-most diagrams of Fig. 2 collide. Both of these difficulties have been treated before in calculations of the $K_L - K_S$ mass difference [5, 6] and the long-distance part of indirect CP violation parameter ϵ_K [7].

It is natural to compute a second-order decay amplitude in Euclidean space by evaluating the matrix element of the usual second-order product of operators which cause the decay:

$$\int_{-\frac{T}{2}}^{\frac{T}{2}} dt_a \langle \pi \nu \bar{\nu} | T \left(O_A(t_a) O_B(t_b) \right) | K \rangle = - \sum_n \left\{ \frac{\langle \pi \nu \bar{\nu} | O_A | n \rangle \langle n | O_B | K \rangle}{M_K - E_n} \left(1 - e^{(M_K - E_n)(\frac{T}{2} - t_b)} \right) \right. \quad (7)$$

$$\left. + \frac{\langle \pi \nu \bar{\nu} | O_B | n \rangle \langle n | O_A | K \rangle}{M_K - E_n} \left(1 - e^{(M_K - E_n)(\frac{T}{2} + t_b)} \right) \right\},$$

where the operators O_A and O_B are replaced by the first-order terms in \mathcal{H}_{eff} given in Eq. (2). The left-hand side is an expression for the decay amplitude that could be extracted from the Euclidean, time-development operator, expanded in powers of G_F . As can be seen from the sum over intermediate states introduced on the right-hand side, this expression contains unwanted transition amplitudes to states of lower energy than the initial K^+ state. These contributions, found in the $\exp\{(M_K - E_n)\frac{T}{2}\}$ terms in Eq. (7), grow exponentially with the integration range T for states $|n\rangle$ with $E_n < M_K$. In time-dependent, Minkowski-space perturbation theory such terms instead oscillate and are eliminated by a proper definition of the large-time limit. Fortunately in a finite volume the resulting discrete, unphysical, exponentially-growing terms can be separately calculated and removed, resulting only in an increased statistical error. In the calculation reported here we evaluate the four-point function on the left-hand side of Eq. (7) and perform these needed subtractions.

The problem of regulating and renormalizing the singular, bilocal, operator products appearing in Eq. (7) has already been solved in the perturbative treatments of this decay where the effective Hamiltonian given in Eq. (2) (which we will use) has been worked out [8]. In this continuum treatment the log-divergent part of bilocal operator product is made finite by dimensional regularization and the $\overline{\text{MS}}$ renormalization scheme. The resulting dependence on the $\overline{\text{MS}}$ renormalization scale $\mu_{\overline{\text{MS}}}$ is canceled by the appropriate counter term which appears in the second-order, four-fermion operator O_0 in Eq. (2). This $\mu_{\overline{\text{MS}}}$ -dependent counter term is chosen so that the full second-order calculation using \mathcal{H}_{eff} correctly reproduces the low energy behavior of the standard model.

For our lattice calculation we follow a closely related strategy which differs from the continuum approach in two respects. First we need not match our effective lattice theory to the complete, standard-model amplitude. Since the continuum, $\overline{\text{MS}}$ -renormalized, effective theory already describes the long-distance behavior of the standard model, we need only match with that formulation. Second, we replace dimensional renormalization by a generalization of the Rome-Southampton, regularization-invariant, RI/SMOM procedure, appropriate for a lattice calculation.

Specifically we begin with the continuum, $\overline{\text{MS}}$ version of Eq. (2). Following standard methods, the local second order operator $O_0^{\overline{\text{MS}}}$ can be easily expressed as a lattice operator times a known coefficient which will depend on $\mu_{\overline{\text{MS}}}$. Likewise the other first-order terms can be also expressed in terms of lattice operators. The new ingredient is our method for representing the $\overline{\text{MS}}$ -renormalized, second-order, bilocal operator on the lattice. Our strategy is summarized by the following equation:

$$\left\{ \int d^4x T \left(O_A^{\overline{\text{MS}}}(x) O_B^{\overline{\text{MS}}}(0) \right) \right\}^{\overline{\text{MS}}} \quad (8)$$

$$= Z_A Z_B \left\{ \int d^4x T \left(O_A^{\text{Lat}}(x) O_B^{\text{Lat}}(0) \right) \right\}^{\text{Lat}} + \left(Z_A Z_B X_{AB}^{\text{Lat} \rightarrow \text{RI}} + Y_{AB}^{\text{RI} \rightarrow \overline{\text{MS}}} \right) O_0^{\overline{\text{MS}}}(0).$$

The left-hand side is an example continuum expression which, together with the easier four-fermion operator $O_0^{\overline{\text{MS}}}$, accurately describes the standard model at low energies. The left-most term on the right-hand side is the corresponding lattice operator. We have introduced the standard renormalization factors Z_A and Z_B that convert the lattice operators into their $\overline{\text{MS}}$ equivalents. Thus, when $x \neq 0$ Eq. (8) is obeyed without the need for the $O_0(0)$ term. We handle the singularity as $x \rightarrow 0$ in two steps. First we add the counter term $Z_A Z_B X_{AB}^{\text{Lat} \rightarrow \text{RI}} O_0$ to convert that product of lattice operators into one which obeys an RI/SMOM condition. In particular we require that a Landau-gauge-fixed Green's function including this bilocal operator and four off-shell, external fermion lines vanishes for specific, non-exceptional external momenta defined at a scale μ_{RI} . Second we use QCD perturbation theory, employed at the large scale $\mu_{\text{RI}} \gg \Lambda_{\text{QCD}}$ to determine the coefficient $Y_{AB}^{\text{RI} \rightarrow \overline{\text{MS}}}$ to convert our RI to the usual $\overline{\text{MS}}$ renormalization of the $x \rightarrow 0$ singularity in the bilocal product.

Finally we mention a further issue arising when Eq. (7) is used in finite volume. As can be seen from that equation, a singularity appears as the energy of a discrete, finite-volume state approaches M_K . Such large, finite-volume corrections are well-understood and can be removed [9].

2. Exploratory lattice QCD calculation

We will now describe a first calculation in which these methods are implemented. We use an RBC/UKQCD $16^3 \times 32$ ensemble with $M_\pi = 420$ MeV, $M_K = 540$ MeV and $1/a = 1.73$ GeV. We use an unphysically light charm quark mass, $m_c(2\text{GeV})^{\overline{\text{MS}}} = 863$ MeV to reduce finite lattice spacing errors. We calculate all relevant diagrams on 800 gauge configurations and employ low-mode deflation using 100 low modes. For each separation between the kaon source and pion sink we perform separate measurements in which the kaon source is placed on each of the 32 time slices. The quarks are treated as domain wall fermions with an extent of 16 in the fifth dimension. The internal lepton is treated as an overlap fermion propagating in an infinite time extent.

For the WW -exchange graphs we evaluate the scalar amplitude F_{WW} [1] which depends on the two Dalitz kinematic variables for this three-body decay. The vector and axial current matrix elements that describe the Z -exchange results are described by familiar, $K13$ -like form factors

$f_+((p_K - p_\pi)^2)$. In analyzing and presenting our long-distance results we ignore what is a likely mild dependence of these quantities on the kinematic variables. This allows us to use P_c of Eq. (1) and the terms of which it is composed to represent matrix elements, treated here as constants. We use an initial kaon which is at rest and study both $\vec{p}_\pi = (0.0414, 0.0414, 0.0414)/a$ and, to determine the contribution of the vector current in Z-exchange case, we also study $\vec{p}_\pi = \vec{0}$.

We present our preliminary results using the quantity $\Delta P_{c,u}$, defined as follows. The continuum result for the decay amplitude is conventionally expressed as the sum of matrix elements of bilocal and local $\overline{\text{MS}}$ operators. The contribution of the bilocal operator (which is the target of our calculation) is typically treated by “integrating out” the charm and up quarks and replacing the bilocal operator with an operator proportional to the four-fermion operator O_0 of Eq. (6). The proportionality constant is determined by equating zero-momentum Green’s functions containing the bilocal and local operators. We will denote the resulting total charm contribution as $P_c^{\text{PT}} = 0.365(12)$ [4], since all of P_c^{PT} is determined perturbatively except for the matrix element of the local operator. Finally, a correction is added to incorporate more refined estimates of the up-quark and other long-distance effects as well as terms suppressed by $(\Lambda_{\text{QCD}}/m_c)^2$, conventionally written as $\delta P_{c,u} = 0.04(2)$ [10].

Here we replace this long-distance correction $\delta P_{c,u}$ by the explicit lattice QCD evaluation of the $\overline{\text{MS}}$ bilocal operator, introducing $\Delta P_{c,u}$ as the result for this bilocal operator matrix element minus the perturbative estimate of that matrix element described above. While $\Delta P_{c,u}$ should be added as a “correction” to P_c^{PT} , it contains a complete evaluation of the bilocal operator matrix element and a term subtracting the standard evaluation of that matrix element found in P_c^{PT} . In Fig. 3 we show the contributions of the WW and Z-exchange graphs as a function of $\mu_{\text{RI}} = \mu_{\overline{\text{MS}}}$. Note the large cancellation between the contributions of these two types of diagrams to $\Delta P_{c,u}$.

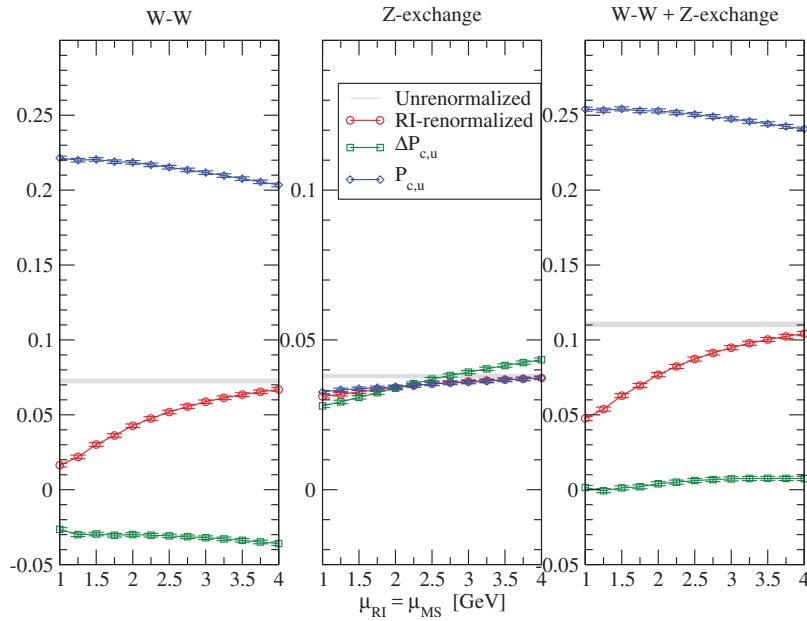


Figure 3: Four quantities are shown: the unrenormalized lattice matrix element of the bilocal operator (gray band); the RI-renormalized version of that same matrix element (red circles); the complete $\Delta P_{c,u}$ result including conversion to $\overline{\text{MS}}$ and subtraction of the conventional bilocal operator matrix element (green squares) and the result for the total charm contribution $P_{c,u}^{\text{PT}} + \Delta P_{c,u}$ (blue diamonds).

3. Conclusion

Our result from this exploratory calculation with unphysical charm and light quark masses is

$$\Delta P_{c,u}(\mu_{\overline{\text{MS}}} = \mu_{\text{RI}} = 2 \text{ GeV}) = 0.0040(13)(32), \quad (9)$$

where the first error is statistical and the second an estimate of the error implied by the residual μ dependence of the complete result: $P_{c,u} = P_{c,u}^{\text{PT}} + \Delta P_{c,u}$. We emphasize that a comparison with the result of Ref. [10] for $\delta P_{c,u}$ is premature and even the large cancellation and subsequent small value for $\Delta P_{c,u}$ may change when the calculation is repeated with physical quark masses. However, this first, complete calculation of these long-distance effects demonstrates that these effects are now practical targets for future work. Accurate results with controlled systematic errors should be attainable in three to four years when adequate computing resources become available.

We thank our colleagues from the RBC and UKQCD collaborations for many helpful discussions. N.H.C and X.F are supported by US DOE grant #DE-SC0011941. A.L is supported by an EPSRC Doctoral Training Centre grant (EP/G03690X/1). A.P and C.T.S are respectively supported by UK STFC grants ST/L000296/1 and ST/L000458/1.

References

- [1] **RBC, UKQCD** Collaboration, N. H. Christ, X. Feng, A. Portelli and C. T. Sachrajda, *Prospects for a lattice computation of rare kaon decay amplitudes II $K \rightarrow \pi \nu \bar{\nu}$ decays*, *Phys. Rev.* **D93** (2016), no. 11 114517 [1605.04442].
- [2] **RBC, UKQCD** Collaboration, N. H. Christ, X. Feng, A. Portelli and C. T. Sachrajda, *Prospects for a lattice computation of rare kaon decay amplitudes: $K \rightarrow \pi \ell^+ \ell^-$ decays*, *Phys. Rev.* **D92** (2015), no. 9 094512 [1507.03094].
- [3] N. H. Christ, X. Feng, A. Juttner, A. Lawson, A. Portelli and C. T. Sachrajda, *First exploratory calculation of the long-distance contributions to the rare kaon decays $K \rightarrow \pi \ell^+ \ell^-$* , 1608.07585.
- [4] A. J. Buras, D. Buttazzo, J. Girrbach-Noe and R. Knegjens, *$K^+ \rightarrow \pi^+ \nu \bar{\nu}$ and $K_L \rightarrow \pi^0 \nu \bar{\nu}$ in the Standard Model: status and perspectives*, *JHEP* **11** (2015) 033 [1503.02693].
- [5] N. Christ, T. Izubuchi, C. Sachrajda, A. Soni and J. Yu, *Long distance contribution to the KL-KS mass difference*, *Phys. Rev.* **D88** (2012) 014508 [1212.5931].
- [6] Z. Bai, N. Christ, T. Izubuchi, C. Sachrajda, A. Soni *et. al.*, *$K_L - K_S$ mass difference from lattice QCD*, *Phys.Rev.Lett.* **113** (2014) 112003 [1406.0916].
- [7] Z. Bai and N. Christ, *Computing the long-distance contributions to ϵ_K* , in *Proceedings, 33rd International Symposium on LatticeField Theory (Lattice 2015)*.
- [8] G. Buchalla, A. J. Buras and M. E. Lautenbacher, *Weak decays beyond leading logarithms*, *Rev. Mod. Phys.* **68** (1996) 1125–1144 [hep-ph/9512380].
- [9] N. H. Christ, X. Feng, G. Martinelli and C. T. Sachrajda, *Effects of finite volume on the KL-KS mass difference*, *Phys. Rev.* **D91** (2015), no. 11 114510 [1504.01170].
- [10] G. Isidori, F. Mescia and C. Smith, *Light-quark loops in $K \rightarrow \pi \nu \text{ anti-}\nu$* , *Nucl. Phys.* **B718** (2005) 319–338 [hep-ph/0503107].